UDC 551.511.33:551.513.1:551.509.313

# Study of Atmospheric Behavior Using A Quasi-Geostrophic, Diabatic, Two-Level Model

C. F. CHOW [1] and E. C. KINDLE [2]—*U.S. Navy Weather Research Facility, Norfolk, Va.*

F. M. VUKOVICH—*Research Triangle Institute, Research Triangle Park, N.C.*

**ABSTRACT**—A simple two-level model was used to explore the effect of diabatic heating in the atmosphere. Nontrivial solutions for the steady-state condition were found only when diabatic heating was allowed. The steady state was characterized by a state of no motion and no growth or decay of energy for a particular wave number. The state of no motion was brought about by a balance between the Rossby motion and the motion produced by the divergence associated with the heating.

The model was used to compute the heating required to account for the observed behavior of individual harmonic components in the atmosphere for the period Jan. 10–14, 1966. The computed magnitudes and positions of the heating waves correlated well with previous results relating to this subject.

## 1. INTRODUCTION

Linearized two-level models have frequently been used to explain the characteristics of atmospheric behavior. In recent years, the diabatic term has been added to these models in attempts to clarify its role. Haltiner (1967) used a nondivergent model to describe the effect of the heating. He found that the heating contributed to the baroclinic instability, but that there was no appreciable difference between the phase speeds in his model and in adiabatic models; that is, the long waves retrogressed at a speed equal to the Rossby speed.

Later, Döös (1969) used a model in which divergence was allowed, to study the role of heating. His solutions consisted of a stationary part and a traveling part. For long waves, the stationary part compared well with observed mean conditions.

In this paper, a simple two-level model is developed that yielded further data concerning the behavior of the atmosphere under the influence of heating. The model allowed for a nonzero, vertically integrated divergence term by letting the heating approach a value of zero at the top level, and being different from zero below. The introduction of net divergence in this manner greatly reduced the retrogression of the long waves and produced a strong coupling between the pressure and thermal waves.

## 2. BASIC ASSUMPTIONS AND MODEL DESCRIPTION

The upper and lower boundaries of the model are 200 mb ($p_4$) and 1000 mb ($p_0$), respectively. In this layer, the mean wind is assumed to increase linearly with decreasing pressure. Diabatic heating is introduced having at most a second-order variation (Taylor series) with pressure, becoming zero at the upper boundary. The vertical velocity, $\omega$, in pressure coordinates is also assumed to have at most a second-order variation with pressure and to be zero at the lower boundary. At the upper boundary, $\omega$ remains free to take on any value and, thus, permits a finite value of the vertically integrated divergence. It is assumed that the horizontal components of the wind velocity can be approximated by a stream function with negligible error (i.e., $u \approx -\partial\psi/\partial y$ and $v \approx \partial\psi/\partial x$). The stream function varies linearly with respect to pressure. All other variations in $y$ are set to zero.

## 3. FORMULATION OF GOVERNING EQUATIONS

The symbols used in the derivation have their common meteorological meanings. However, the symbols not commonly used are shown in table 1.

The primary equation used to describe the behavior of the long waves was the vertical component of the vorticity equation; that is,

$$\frac{\partial\zeta}{\partial t}+u\frac{\partial\zeta}{\partial x}+v\frac{\partial\zeta}{\partial y}+\omega\frac{\partial\zeta}{\partial p}+\beta v=\frac{\partial\omega}{\partial p}(f+\zeta). \tag{1}$$

A thermal vorticity equation was derived by taking the first derivative of eq (1) with respect to pressure. Perturbation principles were applied, and the equations were linearized. Afterwards, the integrals defining the vertical average and thermal quantities were applied. The results were the following equations for the pressure and thermal perturbations:

$$\frac{\partial^3\psi_m'}{\partial t\partial x^2}+\overline{U}_m\frac{\partial^3\psi_m'}{\partial x^3}+\frac{\overline{U}_T}{12}\frac{\partial^3\psi_T'}{\partial x^3}+\beta\frac{\partial\psi_m'}{\partial x}=\left(\frac{\partial\omega}{\partial p}\right)_m' f \tag{2}$$

and

$$\frac{\partial^3\psi_T'}{\partial t\partial x^2}+\overline{U}_m\frac{\partial^3\psi_T'}{\partial x^3}+\overline{U}_T\frac{\partial^3\psi_m'}{\partial x^3}+\beta\frac{\partial\psi_T'}{\partial x}=\left(\frac{\partial^2\omega}{\partial p^2}\right)_m' f\Delta p. \tag{3}$$

[1] Now affiliated with the Center for Experiment Design and Data Analysis, NOAA, Rockville, Md.

[2] Now affiliated with Old Dominion University, Norfolk, Va.

TABLE 1.—*The less common symbols used in this paper*

| | |
|---|---|
| $\psi_m$ | perturbation stream function of the pressure wave |
| $\psi'_T$ | perturbation stream function of the thermal wave |
| $\overline{U}_m$ | mean west–east component of the wind |
| $\overline{U}_T$ | mean west–east component of the thermal wind |
| $\Delta p$ | $p_4-p_0=200$ mb$-1000$ mb$=-800$ mb |
| $H_0$ | heating at 1000-mb surface |
| $\partial^2 H/\partial p^2$ | second derivative of heating |
| $\sigma$ | stability factor |
| $r_1,r_2,r_3$ | system constants involving pressure levels |

$$r_1=\frac{p_4}{\Delta p}\ln\left(\frac{p_4}{p_0}\right)-1$$

$$r_2=p_0^2-p_4^2+2p_0p_4\ln\left(\frac{p_4}{p_0}\right)$$

$$r_3=\frac{\Delta p^2}{12}$$

| | |
|---|---|
| $A_m,B_m$ | Fourier coefficients of the pressure wave |
| $A_T,B_T$ | Fourier coefficients of the thermal wave |
| $h_1,h_2$ | Fourier coefficients of the surface heating wave |
| $\Pi_1,\Pi_2$ | Fourier coefficients of the second derivative heating wave |

$$(\ )_m=\frac{1}{\Delta p}\int_{p_0}^{p_4}(\ )\,dp$$

$$(\ )_T=\int_{p_0}^{p_4}\frac{\partial}{\partial p}(\ )\,dp$$

| | |
|---|---|
| $k$ | wave number units of one over length |

$$k=2\pi n/L$$

| | |
|---|---|
| $L$ | wavelength |
| $n$ | nondimensional wave number |
| $C_m$ | pressure wave speed |
| $C_T$ | thermal wave speed |
| $\alpha_m$ | phase angle of pressure wave |
| $\alpha_T$ | phase angle of thermal wave |
| $\alpha_H$ | phase angle of surface heating wave |
| $\alpha_{H\rho}$ | phase angle of second derivative heating wave |
| $a_m$ | amplitude of pressure wave |

$$a_m^2=A_m^2+B_m^2$$

| | |
|---|---|
| $a_T$ | amplitude of thermal wave |

$$a_T^2=A_T^2+B_T^2$$

| | |
|---|---|
| $h$ | amplitude of surface heating wave |

$$h^2=h_1^2+h_2^2$$

| | |
|---|---|
| $\Pi$ | amplitude of second derivative heating wave |

$$\Pi^2=\Pi_1^2+\Pi_2^2$$

The expressions for the divergence and for the vertical velocity were derived from the first law of thermodynamics; that is,

$$\omega=-\frac{1}{\sigma}\left(\frac{R}{pc_p}H+\frac{\partial}{\partial t}\frac{\partial\phi}{\partial p}+u\frac{\partial}{\partial x}\frac{\partial\phi}{\partial p}+v\frac{\partial}{\partial y}\frac{\partial\phi}{\partial p}\right)$$

where $\phi$ is the geopotential and for this study the approximation $\phi\approx f\psi$ was employed, and $H$ is the rate of heating per unit mass. The heating rate was assumed to have, at most, a second-order variability with pressure. A Taylor expansion was used to describe this variability. Application of the upper boundary condition, $H=0$ at $p=20$ cb, allowed us to substitute for the first-order term so that the expression for the heat term was

$$H=H_0\left[1-\frac{(p-p_0)}{\Delta p}\right]+\frac{1}{2}\frac{\partial^2 H}{\partial p^2}[(p-p_0)^2-\Delta p(p-p_0)].$$

To derive the $\omega$-equation, we applied perturbation principles to the above expression and the resulting equation was linearized. Then the averaging integral was applied. The divergence equation was derived by taking the first derivative of the first law of thermodynamics with respect to pressure, applying perturbation principles, linearizing, and applying the averaging integral. The resulting expressions for the $\omega$-equation and the divergence equation were, respectively,

$$\omega'_m=\frac{f}{\sigma\Delta p}\left(\frac{\partial\psi'_T}{\partial t}+\overline{U}_m\frac{\partial\psi'_T}{\partial x}-\overline{U}_T\frac{\partial\psi'_m}{\partial x}\right)+\frac{RH_0}{\Delta p\sigma c_p}r_1+\frac{r_2}{4\Delta p\sigma c_p}\frac{\partial^2 H}{\partial p^2} \tag{4}$$

and

$$\left(\frac{\partial\omega}{\partial p}\right)'_m=-\frac{RH_0}{\Delta p\sigma c_p p_0}. \tag{5}$$

For eq (5), we assumed that

$$\frac{1}{\Delta p}\int_{p_0}^{p_4}\left[\frac{\partial}{\partial p}\left(\frac{\partial}{\partial t}\frac{\partial\phi}{\partial p}+\mathbf{V}\cdot\nabla\frac{\partial\phi}{\partial p}\right)\right]dp=0.$$

Equation (5) poses a constraint on the atmosphere; that is, the mean divergence is a result of the heating alone, which requires that the temperature difference between top and bottom of the atmosphere remains a constant following the motion. This is accomplished by making the total change in temperature at the surface due to heating equivalent to the total change in temperature at the top of the atmosphere due to the work done in compression or expansion. Though this was a very limiting constraint, we believe that, as a first approximation, the retention of the previously neglected net divergence through heating alone lends a degree of truth to the model and will relate some aspects of the role of diabetic heating in the atmosphere.

To find an expression for the second derivative of $\omega$, we assumed that $\omega$ could be expressed about some pressure level $p_L$ by

$$\omega'=\omega'_L+\left(\frac{\partial\omega'}{\partial p}\right)_L(p-p_L)+\left(\frac{\partial^2\omega'}{\partial p^2}\right)_L\frac{(p-p_L)^2}{2}.$$

Employing the lower boundary condition that $\omega=0$ at $p=p_0$, and integrating over increments of $p_L$, we obtained

the following expression:

$$\left(\frac{\partial^2\omega'}{\partial p^2}\right)_m=\frac{1}{r_3}\left[\frac{\Delta p}{2}\left(\frac{\partial\omega'}{\partial p}\right)_m-\omega'_m\right]. \quad (6)$$

Substitution of eq (4)–(6) into eq (2) and (3) yielded the following prediction equations:

$$\frac{\partial}{\partial t}\frac{\partial^2}{\partial x^2}\psi'_m+\overline{U}_m\frac{\partial^3}{\partial x^3}\psi'_m+\frac{\overline{U}_T}{12}\frac{\partial^3}{\partial x^3}\psi'_T+\beta\frac{\partial}{\partial x}\psi'_m=m_1H_0 \quad (7)$$

$$\frac{\partial}{\partial t}\left(\frac{\partial^2}{\partial x^2}+m_4\right)\psi'_T+\overline{U}_T\left(\frac{\partial^2}{\partial x^2}-m_4\right)\frac{\partial}{\partial x}\psi'_m+\overline{U}_m\left(\frac{\partial^2}{\partial x^2}+m_4\right)\frac{\partial}{\partial x}\psi'_T+\beta\frac{\partial}{\partial x}\psi'_T=m_2H_0+m_3\frac{\partial^2H}{\partial p^2} \quad (8)$$

where

$$m_1=\frac{-fR}{\Delta p\sigma c_p p_0},$$

$$m_2=\frac{\Delta p m_1 p_0}{r_3}\left(\frac{\Delta p}{2p_0}+r_1\right),$$

$$m_3=\frac{m_1p_0}{4}\frac{r_2}{r_3},$$

and

$$m_4=\frac{f^2}{r_3\sigma}.$$

A solution to eq (7) and (8) was obtained by letting

$$\psi'_m=\sum(A_m\cos kx+B_m\sin kx),$$

$$\psi'_T=\sum(A_T\cos kx+B_T\sin kx),$$

$$H_0=\sum(h_1\cos kx+h_2\sin kx),$$

and

$$\frac{\partial^2H}{\partial p^2}=\sum(\Pi_1\cos kx+\Pi_2\sin kx).$$

This yielded the following system of prediction equations:

$$\begin{aligned}
&\frac{\partial A_m}{\partial t}+0+T_1B_m+T_2B_T=H_1,\\
&0+\frac{\partial A_T}{\partial t}+T_3B_m+T_4B_T=H_2,\\
&-T_1A_m-T_2A_T+\frac{\partial}{\partial t}B_m+0=H_3,\\
&-T_3A_m-T_4A_T+0+\frac{\partial}{\partial t}B_T=H_4
\end{aligned} \quad (9)$$

and

where

$$T_1=\left(\overline{U}_m-\frac{\beta}{k^2}\right)k,$$

$$T_2=\frac{\overline{U}_Tk}{12},$$

$$T_3=\overline{U}_Tk\frac{(k^2+m_4)}{(k^2-m_4)},$$

$$T_4=\left(\overline{U}_m-\frac{\beta}{(k^2-m_4)}\right)k,$$

$$H_1=-\frac{m_1}{k^2}h_1,$$

$$H_2=\frac{-1}{k^2-m_4}(m_2h_1+m_3\Pi_1),$$

$$H_3=-\frac{m_1}{k^2}h_2,$$

and

$$H_4=\frac{-1}{k^2-m_4}(m_2h_2+m_3\Pi_2).$$

Since eq (7) and (8) are linear, there is no loss of generality if we consider individual wave components as in eq (9).

From the above equations, the expressions for the phase speeds for the pressure and thermal waves were derived; they are,

$$C_m=\overline{U}_m-\frac{\beta}{k^2}+\frac{\overline{U}_T}{12}\frac{a_T}{a_m}\cos(\alpha_T-\alpha_m)-\frac{m_1}{k^3}\frac{h}{a_m}\sin(\alpha_H-\alpha_m) \quad (10)$$

and

$$C_T=\overline{U}_m-\frac{\beta}{k^2-m_4}+\overline{U}_T\frac{a_m}{a_T}\frac{(k^2+m_4)}{(k^2-m_4)}\cos(\alpha_T-\alpha_m)-\frac{m_2}{k(k^2-m_4)}\frac{h}{a_T}\sin(\alpha_H-\alpha_T)-\frac{m_3\Pi}{k(k^2-m_4)}\frac{\sin(\alpha_{Hp}-\alpha_T)}{a_T}. \quad (11)$$

For the case of adiabatic motion ($h=\Pi=0$), these phase speeds are consistent with those formulated in other two-level models. In the adiabatic case and for long waves, the Rossby term controls the pressure wave speed. The remaining term, which is a baroclinic term, is small in comparison; thus, the long pressure waves will retrogress. The Rossby term is modified by the stability of the atmosphere in the expression for the thermal wave speed. The stability term is two orders of magnitude larger than the square of the wave number for long waves, which considerably reduces the retrogression or even produces progression of the long thermal waves for certain westerly wind speeds. This is identical to the disjointed behavior of the two waves described by Wiin-Nielsen (1961). The effect of the heating will be discussed later.

The time rate of change of kinetic energy of the two waves are given by the following:

$$\frac{1}{2}\frac{\partial}{\partial t}a_m^2=\frac{\overline{U}_T}{12}ka_ma_T\sin(\alpha_m-\alpha_T)-\frac{m_1}{k^2}a_mh\cos(\alpha_m-\alpha_H) \quad (12)$$

and

$$\frac{1}{2}\frac{\partial}{\partial t}a_T^2=\frac{1}{k^2-m_4}[\overline{U}_Ta_ma_Tk(k^2+m_4)\sin(\alpha_T-\alpha_m)-m_2ha_T\cos(\alpha_T-\alpha_H)-m_3\Pi a_T\cos(\alpha_T-\alpha_{Hp})]. \quad (13)$$

For the adiabatic case, these expressions are also consistent with those formulated in other two-level models. Note that, if we assume that there is no perturbation energy in this system in the initial state, the total growth of kinetic energy in the model would come directly from the effect of heating and indirectly from the subsequent baroclinic

growth that would ensue; there could never be a transfer of energy from the mean motion to the perturbation motion in a linear model.

The characteristic equation for each of the four Fourier coefficients was derived through simultaneous solution of eq (9). It takes the form

$$\left(\frac{d^4}{dt^4}+a\frac{d^2}{dt^2}+b\right)\xi=G(H,\,t) \tag{14}$$

where

$$a=T_1^2+T_4^2+2T_3T_2,$$

$$b=(T_1T_4-T_2T_3)^2,$$

and $\xi$ is a dummy parameter that is replaced by any of the Fourier coefficients. The parameter $G$ is the forcing function, which is a function of heating and time and involves, at most, third-order derivatives of the heating. The exact expression for $G$ will depend on which coefficient replaces $\xi$

The particular solution for eq (14), under the condition that the forcing function is time independent and with the boundary conditions $\xi=0$, $\partial\xi/\partial t=G_1(H,0)$, $\partial^2\xi/\partial t^2=G_2(H,0)$, and $\partial^3\xi/\partial t^3=G_3(H,0)$ when $t=0$, is

$$\xi=\frac{G(H,0)}{b}\left\{1+\frac{1}{2\sqrt{F}}\left[(a-\sqrt{F})\cos\sqrt{\frac{a+\sqrt{F}}{2}}t-(a+\sqrt{F})\right.\right.$$

$$\left.\times\cos\sqrt{\frac{a-\sqrt{F}}{2}}t\right]\Bigg\}+\frac{1}{\sqrt{F}}\Bigg\{\frac{G_1(H,0)}{2}\left[(a+\sqrt{F})\sin\sqrt{\frac{a-\sqrt{F}}{2}}t\right.$$

$$\left.-(a-\sqrt{F})\sin\sqrt{\frac{a+\sqrt{F}}{2}}t\right]$$

$$+G_2(H,0)\left[\cos\sqrt{\frac{a-F}{2}}t-\cos\sqrt{\frac{a+\sqrt{F}}{2}}t\right]$$

$$+G_3(H,0)\left[\frac{\sin\sqrt{\frac{a-\sqrt{F}}{2}}t}{\sqrt{\frac{a-\sqrt{F}}{2}}}-\frac{\sin\sqrt{\frac{a+\sqrt{F}}{2}}t}{\sqrt{\frac{a+\sqrt{F}}{2}}}\right]\Bigg\}$$

where $F=a^2-4b$. The initial values of the derivatives, $G_1(H,0)$, $G_2(H,0)$, and $G_3(H,0)$, can be derived from eq (9) by taking derivatives of these expressions and setting the coefficients equal to zero. They are time independent since the heating is time independent. The expressions are:

$$\text{if } \xi=A_m,$$

$$G_1(H,\,0)=H_1,$$

$$G_2(H,\,0)=-(T_1H_3+T_2H_4),$$

and

$$G_3(H,\,0)=-T_1(T_1H_1+T_2H_4)-T_2(T_3H_1+T_4H_2);$$

$$\text{if } \xi=B_m,$$

$$G_1(H,\,0)=H_3,$$

$$G_2(H,\,0)=T_1H_1+T_2H_2,$$

and

$$G_3(H,\,0)=-T_1(T_1H_3+T_2H_4)-T_2(T_3H_3+T_4H_4);$$

$$\text{if } \xi=A_T,$$

$$G_1(H,\,0)=H_2,$$

$$G_2(H,\,0)=-(T_3H_3+T_4H_4),$$

and

$$G_3(H,\,0)=-T_3(T_1H_1+T_2H_2)-T_4(T_3H_1+T_4H_2);$$

and

$$\text{if } \xi=B_T,$$

$$G_1(H,\,0)=H_4,$$

$$G_2(H,\,0)=T_3H_1+T_4H_2,$$

and

$$G_3(H,\,0)=-T_3(T_1H_3+T_2H_4)-T_4(T_3H_3+T_4H_4).$$

The diabatic forcing function, $G(H,\,0)/b$, will be discussed later.

The solution has a forced response due to heating and a transient response due to convective and dynamic transports. It has, provided $\sqrt{F}$ is real and $a>0$, oscillations about the forced response with two periods that are related to the Rossby motion of the pressure and thermal waves (Vukovich and Chow 1968*a*). This compares favorably with the solution of Döös (1969). Note that the solution is zero if heating is zero.

## 4. STABILITY CRITERIA

The stability criteria for the fourth-order differential equation are derived from the eigenfunction,

$$m=\pm\sqrt{-\frac{a}{2}\pm\frac{1}{2}\sqrt{F}},$$

where $m$ is the eigenvalue of the differential equation. Since $b\geq 0$ always, then if $F>0$ and $a>0$, $m$ will be imaginary and the waves are neutral. However, if $F<0$, the expression in the first radical will be complex, the solution will have a positive real part, and the waves will be unstable. The values for $F$ versus wave number were computed for mean winds of 20 and 40 m/s, thermal winds of 10, 20, 30, and 40 m/s, 45° latitude, and a standard atmospheric lapse rate. The results are given in figures 1 and 2.

Figure 1 yields the stability criteria for a mean wind of 20 m/s. The numbers in parentheses are the thermal wind speeds. Only the regions in the neighborhood of the unstable waves are plotted. Wave numbers greater than 15 are always neutral for the parameters used. With a thermal wind of 10 m/s or less, all waves are neutral. For thermal wind speeds somewhere between 10 and 20 m/s, a transition occurs and a finite band of long waves becomes unstable ($F<0$). In general, the unstable wave band is centered about wave number 8. The effect of increasing the thermal wind is to broaden the band of unstable

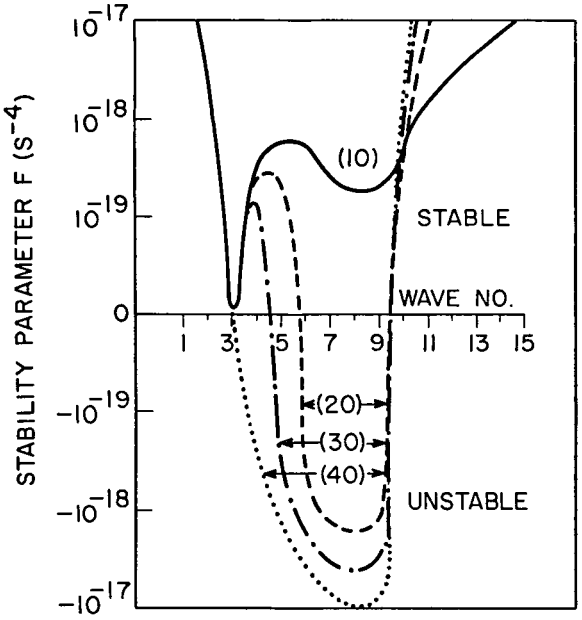


FIGURE 1.—The parameter, $F$, versus wave number for $\overline{U}_m$ of 20 m/s. The values of $\overline{U}_T$ (m/s) are in parentheses. When $F>0$, the waves are neutral, and when $F<0$, the waves are unstable.

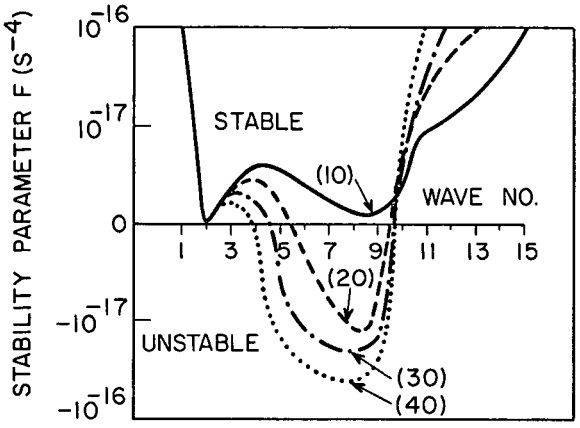


FIGURE 2.—Same as figure 1 for $\overline{U}_m$ of 40 m/s.

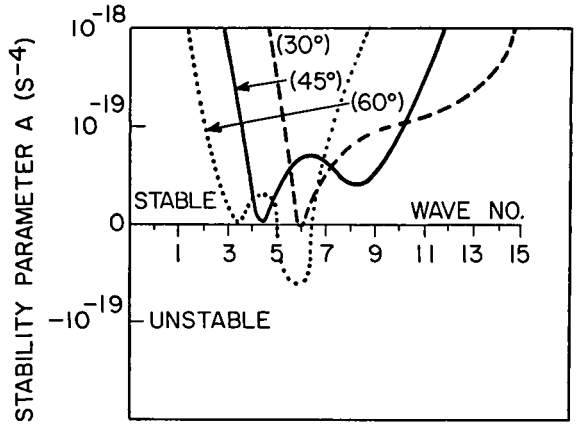


FIGURE 3.—The parameter, $F$, versus latitude for $\overline{U}_m$ and $\overline{U}_T$ of 10 m/s. The latitudes (deg.) are in parentheses. The waves are unstable when $F<0$.

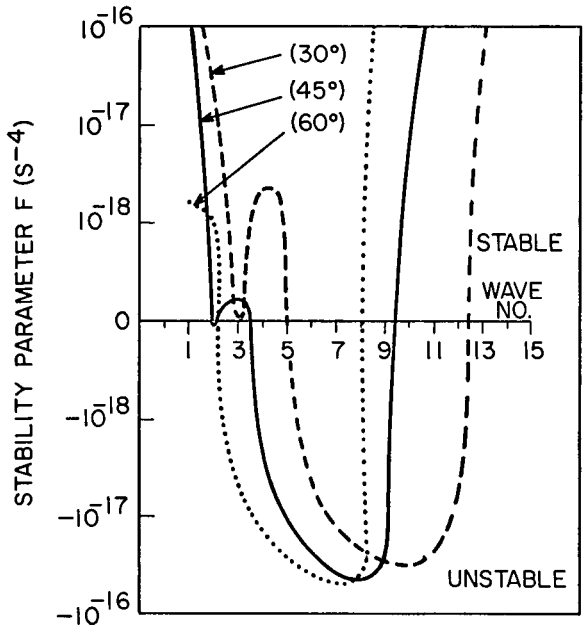


FIGURE 4.—Same as figure 3 for $\overline{U}_m$ and $\overline{U}_T$ of 40 m/s.

waves. Increasing the mean wind speed to 40 m/s does not change the nature of the solution appreciably (fig. 2). These solutions are in general agreement with those of Charney (1947), Gates (1961), and Ogura (1957).

Figures 3 and 4 yield the effect of varying latitude on the stability parameter, $F$. Figure 3 gives this variation for a mean wind speed of 10 m/s and a thermal wind speed of 10 m/s. The standard atmospheric lapse rate is also employed for these computations. The numbers in the parentheses are the latitudes. From 30° to 45° latitude, all waves are neutral. However, between 45° and 60° latitude, instability is formed in a narrow band centered about wave number 6 because of the reduced effectiveness of the Rossby parameter. For mean and thermal wind speeds of 40 m/s, increasing the latitude shifts the band of unstable waves toward lower wave numbers (fig. 4). The number of unstable waves also decreases with increasing latitude.

## 5. STEADY-STATE SOLUTION AND THE FORCED RESPONSE

If heating were everywhere zero, the steady-state solution for the Fourier coefficients in eq (9) would be trivial; that is, the coefficients must be identically zero. In this study, the nontrivial solution can only arise if heating exists. A steady state can also be obtained when the atmosphere is influenced by topography. In essence, to obtain a steady state, the atmosphere in the linear problem must be under the influence of a forcing function. There remains the possibility that a steady state may be achieved without a forcing function if nonlinear interactions are allowed.

The existence of a steady-state solution indicates that the heating, and the subsequently induced baroclinicity, is balancing the Rossby motion (not possible in adiabatic models) and that energy in either the pressure or thermal wave is not being created by either the baroclinic or the

diabatic forces. This state usually characterizes the ultralong waves. The steady-state solutions are

$$A_m=\frac{T_2H_3-T_4H_4}{T_1T_4-T_2T_3},$$

$$B_m=\frac{T_4H_1-T_2H_2}{T_1T_4-T_2T_3},$$

$$A_T=\frac{T_3H_3-T_1H_4}{T_1T_4-T_2T_3},$$

and

$$B_T=\frac{T_1H_2-T_3H_1}{T_1T_4-T_2T_3}.$$

These solutions are identical to the forced response $[G(H,0)/b]$ in eq (15) when the heating is time independent.

One must remember that a steady state cannot be attained without the influence of friction. Examination of eq (15) shows that the transient response is nondissipative, so that steady-state solutions will never be achieved. However, we believe that studying the steady-state solution will yield insight into the quantitative behavior of the atmosphere, since the steady-state solution is identical with the forced response when the forcing function is independent of time.

Characteristic heating amplitudes consistent with the experiments of Döös (1961) and Ninomiya (1964) were chosen to compute corresponding steady-state amplitudes and phases for the pressure and thermal waves. Döös and Ninomiya determined tha magnitude of synoptic diabatic heating near the earth's surface. Döös arrived at a value of approximately $10\times10^{-5}$J·g$^{-1}$·s$^{-1}$ and Ninomiya obtained a value of $6\times10^{-5}$ J·g$^{-1}$·s$^{-1}$. Ninomiya's computations were for the very intense winter heating over the Sea of Japan, but his value was less than that of Döös because it was a 10-day average value.

These heating computations provided specific values of surface heating over specific areas and reflected the sum of all harmonics for a given latitude. Therefore, a value considerably less than the values they computed should be used for the heating amplitude of a single harmonic. For the following computations, a value exactly one-tenth that of Döös ($1.0\times10^{-5}$ J·g$^{-1}$·s$^{-1}$) was chosen for a characteristic amplitude of a given harmonic.

To simplify the computations, we assumed the phase angle of the heating waves to be zero. All of the phase angles would be referred to the location of the heating wave. Furthermore, the heating is assumed to vary linearly with pressure (i.e., $\partial^2H/\partial p^2=0$). By these assumptions, the thermal and pressure waves would have to have a phase angle of $\pm90°$ with respect to the heating wave, and they would have to be either in phase or 180° out of phase with respect to each other [i.e., $A_T=A_m=0$ because $h_2=(\partial^2H/\partial p^2)=0$]. One can see that, under these conditions, the baroclinic term and the heating term contribute their maximum effect to the speed of the pressure and thermal waves [eq (10) and (11)]. The phase relationships create a zero time derivative for the kinetic energy of both waves [eq (12) and (13)].

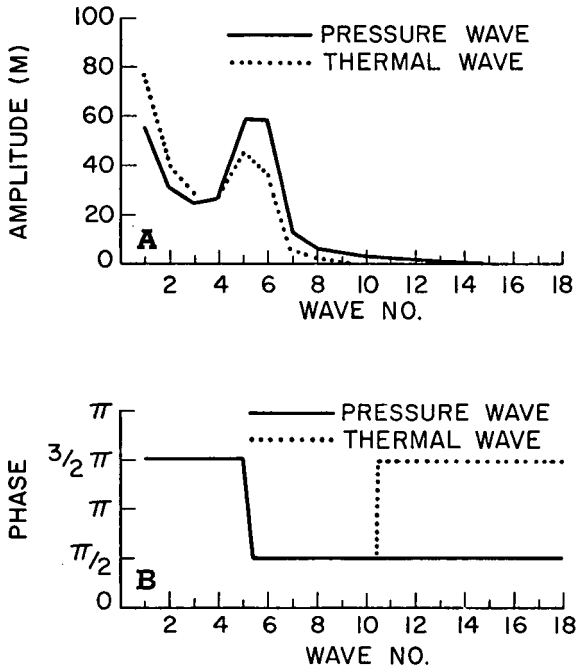


FIGURE 5.—(A) amplitude (m) and (B) phase of the pressure and thermal waves at 45° latitude for $\bar{U}_m$ and $\bar{U}_T$ of 10 m/s.

Figure 5A yields the amplitude spectrum for the pressure and thermal waves when the mean and thermal wind were both 10 m/s. The latitude was 45°. The most excited mode is wave number 1. A secondary maximum, found at wave number 5 for both waves, is due to the addition of heat at a frequency nearly equal to one of the natural frequencies of the system. If friction were included in the model, resonance would be prevented and infinite amplitudes would not occur. However, large, bounded perturbations would still exist at wave numbers in the near vicinity of nonfrictional resonance (Smagorinsky 1953). This result is in contrast with that of Derome and Wiin-Nielsen (1971) in which no effects of resonance were found in their heating model. However, differences may be due to parameters used.

The pressure and thermal waves are in phase (fig. 5B) up to wave number 11, indicating that the pressure perturbation increases with decreasing pressure along the local vertical for these wave numbers. In an earlier study by Smagorinsky (1953), he found that the perturbations decreased with decreasing pressure at 35° latitude, but increased at 60° latitude. Derome and Wiin-Nielsen (1971) and Murakami (1967) found that only the ultralong waves increased with decreasing pressure. In the present study, the perturbation decreases with decreasing pressure only after wave number 10.

When the waves are displaced upstream of the heating wave (waves 1–6), surface heating is found in regions of southward geostrophic flow, and surface cooling occurs in regions of northward geostrophic flow in the Northern Hemiphere. This is consistent with the concept that air from the polar regions is warmed moving southward, and tropical air is cooled during its northward movement. However, when the waves are displaced downstream of

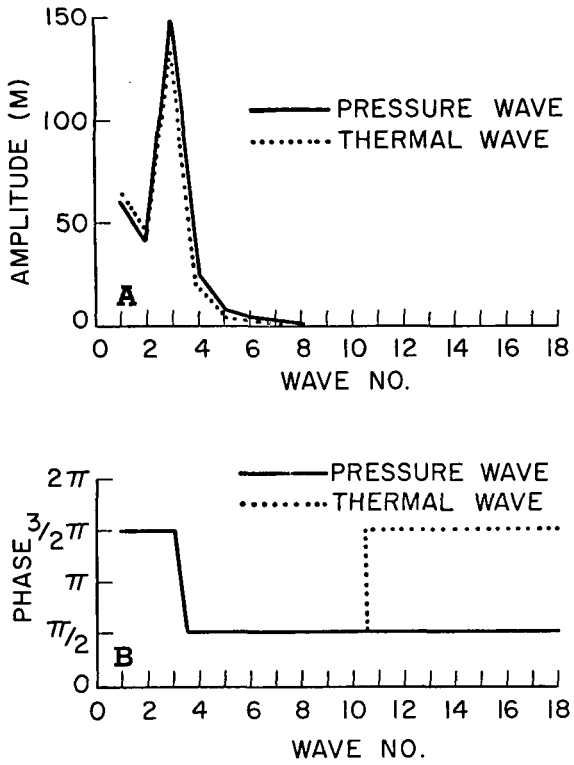


FIGURE 6.—Same as figure 5 for $\overline{U}_m$ and $\overline{U}_T$ of 30 m/s.

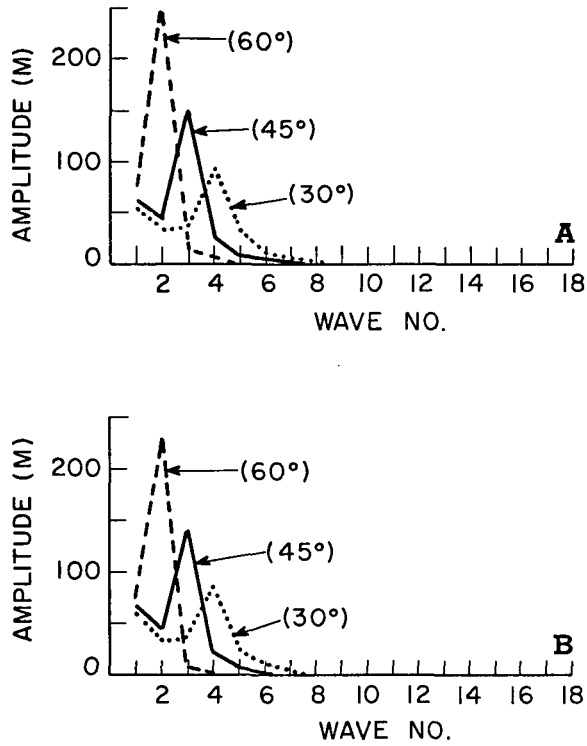


FIGURE 7.—(A) pressure wave and (B) thermal wave amplitudes versus latitude for $\overline{U}_m$ and $\overline{U}_T$ of 30 m/s.

the heating wave (waves 6–11), the correlation between the geostrophic transport and the heating does not occur. In developing the solution of eq (14), we assumed the heating to be time independent. This means that neither the amplitude nor the phase changes. Consequently, the heating is fixed in space and is due, therefore, to the surface temperature distribution and not to the geostrophic flow.

Increasing both the mean and thermal wind to 30 m/s decreases the wave number of nonfrictional resonance to 3 (fig. 6A), which is also the most excited mode. The phase relationship (fig. 6B) is the same as before except that the transition from upstream to downstream displacement is now found around wave number 3.

The effect of varying the latitude on the pressure and thermal wave amplitude is given in figure 7. The mean and thermal wind are both 30 m/s for these calculations. Nonfrictional resonance is found near wave number 4 for 30° latitude, near wave number 3 for 45°, and near wave number 2 for 30°. Apparently, increasing the latitude decreases the wave number at which nonfrictional resonance is found.

Fujita (1956) has shown that the ultralong waves (wave nos. 1–3) are in quasi-steady state. The pressure wave amplitudes he found were 50 m for wave number 1 and 60 m for wave numbers 2 and 3. In the present study, the forced response, which is also the steady-state solution, yielded pressure amplitudes of 55 m for wave number 1, 30 m for wave number 2, and 25 m for wave number 3. Though a steady-state solution is not possible in a nondissipative model, these pressure wave amplitudes, which are indicative of amplitudes to be expected under the action of friction, indicate that a heating amplitude of as little as $1.0\times10^{-5}$J·g$^{-1}$·s$^{-1}$ is sufficient to stop the retrogression that usually characterizes these waves.

## 6. PHYSICAL EXPERIMENT

The heating distribution required to account for the observed behavior of individual harmonic components in the atmosphere for the period Jan. 10–14, 1966, was computed. The Fourier coefficients for the pressure and thermal waves were computed for 30°, 45°, and 60°N latitude. For each wave number and each latitude, the derived amplitudes and their time derivatives were substituted into eq (9), and the surface heating necessary to bring about this observed behavior was computed.

Figure 8 yields the resultant surface heating distribution after summing over wave numbers 1, 2, and 3 at 45°N latitude. The resultant pressure distribution is also depicted. Negative values correspond to low pressure and positive values, to high pressure. Both sets of data represent an average over the period.

The order of magnitude of the heating is comparable to values derived by Döös (1961) and Ninomiya (1964). The fact that the present magnitudes are less than theirs is to be expected since these results represent the sum of three wave numbers and theirs represent the sum of all wave numbers. The pressure wave lags the heating by approximately 90°, and the pressure and thermal waves are approximately in phase (not shown in figure), which is indicative of a quasi-steady-state condition that normally characterizes these waves. Heating is found in regions of southward geostrophic flow, and cooling, in regions of northward geotrophic flow. The figure shows two heating regions centered over eastern Asia and eastern

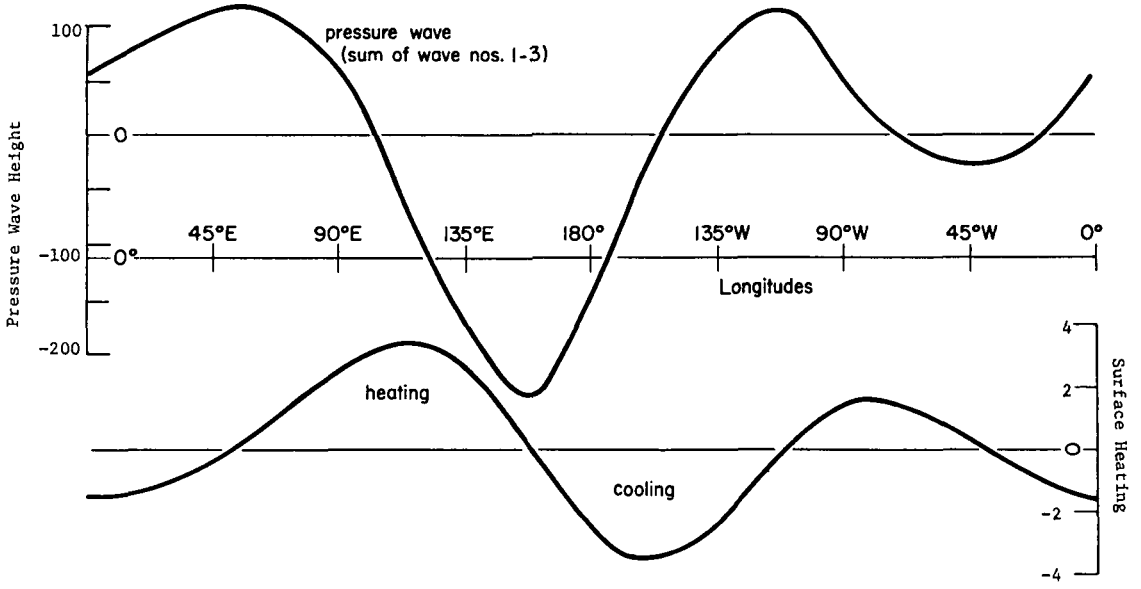


FIGURE 8.—The longitudinal distribution of the pressure wave height (m) and the surface heating ($10^{-5}$ J·g$^{-1}$·s$^{-1}$) at 45°N summing wave numbers 1–3 and averaging over the period Jan. 10–14, 1966.

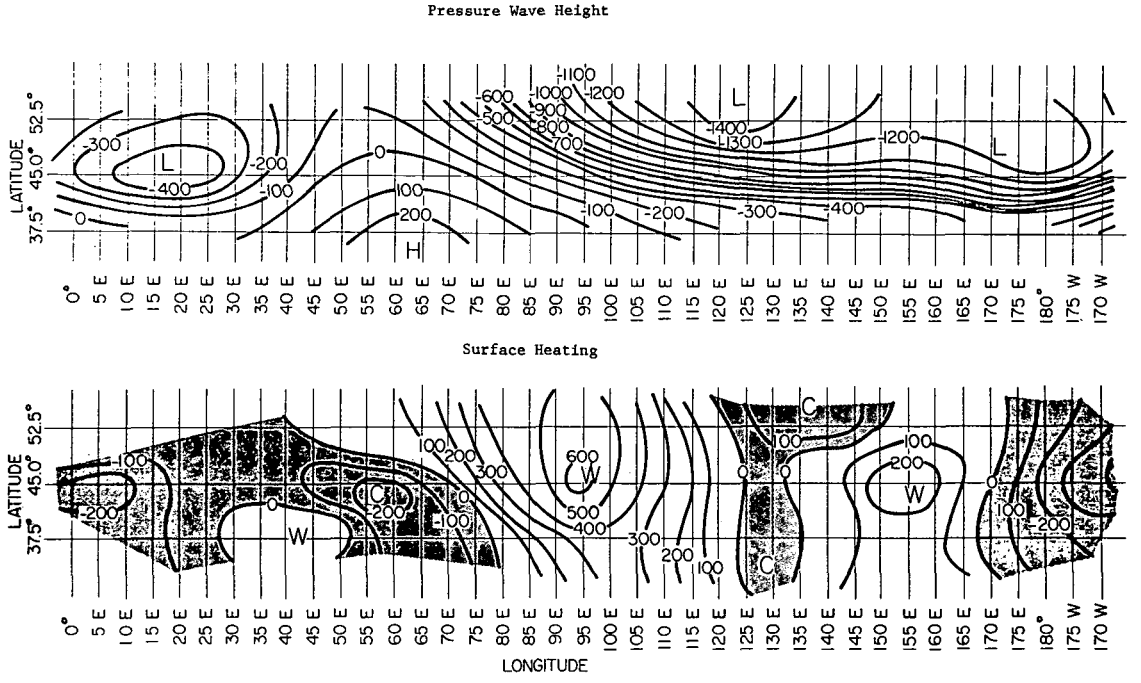


FIGURE 9.—Analysis of height distribution (ft) of the pressure wave and the surface heating ($10^{-7}$ J · g$^{-1}$ · s$^{-1}$) in the latitude belt 30°–60°N, summing wave numbers 1–6 and averaging over the period Jan. 10–14, 1966, for the Eastern Hemisphere.

North America and two cooling regions centered over the east-central Pacific Ocean and western Europe. The maximum heating (approx. $3.0\times10^{-5}$ J·g$^{-1}$·s$^{-1}$) is found over eastern Asia. The location of the pressure troughs and ridges compares well with those found by Fujita (1956), which demonstrates the consistency of these waves. Because the heating is not steady state, heating zones must be fixed features of the flow associated with these waves.

The surface heating distribution that is derived by summing over wave numbers 1–6 and the corresponding pressure distribution for all latitudes are represented in figures 9 and 10. The values are averages over the period as before. Again, the magnitude of the heating compares well with the values given by Döös and Ninomiya. The phase difference between the two waves varies markedly, indicative of non-steady-state conditions. This should occur since waves that fall within the unstable category are included in the summation. The high frequency of cooling and heating centers is expected, since the pressure distribution indicates marked variations in the flow.

The surface heating distribution determined by summing wave numbers 1–9 for all latitudes is represented in figure 11. Only longitudes 55°W to 115°W are shown. Again, the

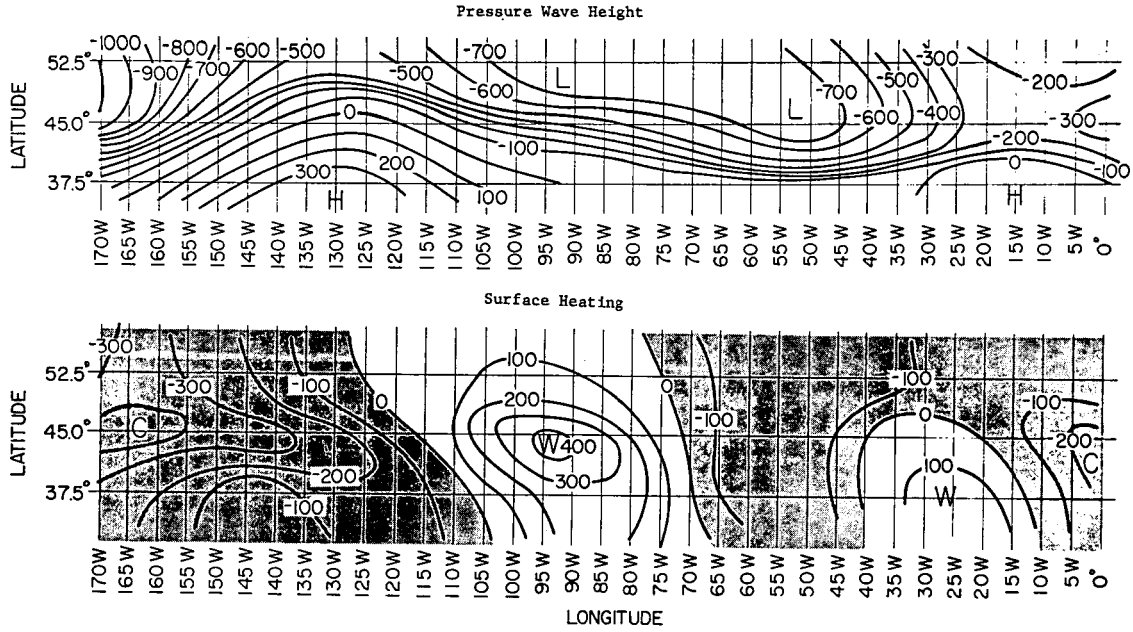


FIGURE 10.—Same as figure 9 for the Western Hemisphere.

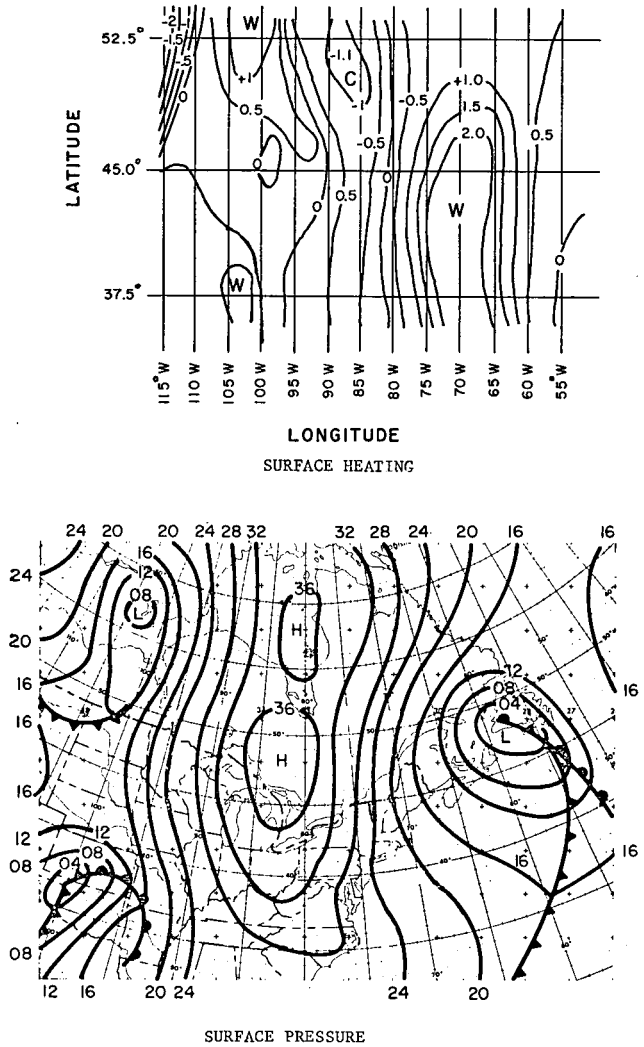


FIGURE 11.—Surface pressure analysis (mb) of the eastern part of North America for 0600 GMT, Jan. 12, 1966, and the surface heating analysis ($10^{-4}$ J · $g^{-1}$ · $s^{-1}$) of eastern North America, summing wave numbers 1–9 and averaging over the period Jan. 10–14, 1966.

values are averages over the period. Also shown in the figure is the 0600 GMT surface pressure chart for the region for Jan. 12, 1966. The maximum heating is twice that found by Döös. The correlation between zones of heating and cooling and zones of northward and southward geostrophic flow at the surface is remarkable considering the simplicity of the model.

## 7. CONCLUSIONS

The general nature of the solution obtained in this study has similar characteristics to that found by Döös (1969); that is, the solution consists of a forced response and a transient response. The transient response contains two response periods that are associated with the Rossby motion of the pressure and thermal wave (Vukovich and Chow 1968*a*). The time-independent, forced response is shown to be the steady-state solution, and a nontrivial steady-state solution is possible if heating existed.

Using amplitudes of $1.0 \times 10^{-5}$ J·$g^{-1}$·$s^{-1}$ for surface heating, we computed steady-state pressure wave amplitudes. These amplitudes compare well with observational data, which indicates that surface heating perturbations with amplitudes as little as $1.0 \times 10^{-5}$ J·$g^{-1}$·$s^{-1}$ are sufficient to compensate for the retrogression of the long waves produced by the Rossby motion.

If heat is added to the atmosphere at all frequencies, the most excited wave number for both the pressure and thermal waves, in most cases, corresponds to that wave number nearest the natural frequency of the system. Friction produces bounded amplitudes in the near vicinity of the resonance frequency. The wave number at which resonance occurs decreases as the mean and thermal wind speed increases and as the latitude increases. For the cases studied, the pressure and thermal waves are in phase and are displaced upstream or downstream 90° from the heating wave for wave numbers less than 11. The perturba-

tions, therefore, increase with decreasing pressure. For wave numbers 11 or greater, the thermal and pressure wave are 180° out of phase and the perturbations decrease with decreasing pressure.

The magnitudes of heating computed in the physical experiment compare well with those found by other researchers (Döös 1961, Ninomiya 1964). The ultralong waves (wave nos. 1–3) satisfy the steady-state criteria. The positions of the pressure troughs and ridges compare well with those found by Fujita (1956). Two heating regions and two cooling regions were found. These regions are directly correlated to the geostrophic flow, which is consistent with the results of Kindle et al. (1967) and Vukovich and Chow (1968*b*). The heating regions are located over eastern Asia and eastern North America, and the cooling regions are found over the east-central Pacific Ocean and western Europe. Since these waves are in quasi-steady state and the heating varies with time, the heating patterns must be fixed features of the flow.

When the results of the calculations for shorter wave heating were included in the analysis, the characteristics of the steady-state solution no longer existed. This was to be expected since wave numbers were now included which fell within the category of baroclinically unstable waves.

## ACKNOWLEDGMENTS

The research was supported, in part, by the Air Force Cambridge Research Laboratories under Contract AF 19(628)–5834. Meteorological data for physical experiments were obtained from the Global Weather Center, Offutt Air Force Base, Nebr.

## REFERENCES

Charney, Jule G., "The Dynamics of Long Waves in a Baroclinic Westerly Current," *Journal of Meteorology*, Vol. 4 No. 5, Oct. **1947**, pp. 135–162.

Derome, Jacques, and Wiin-Nielsen, A., "The Response of a Middle-Latitude Model Atmosphere to Forcing by Topography and Stationary Heat Sources," *Monthly Weather Review*, Vol. 99, No. 7, July **1971**, pp. 564–576.

Döös, Bo R., "The Scale of Non-Adiabatic Heating as a Factor in Cyclogenesis," *Journal of Meteorology*, Vol. 18, No. 1, Feb. **1961**, pp. 1–8.

Döös, Bo R., "The Influence of the Large-Scale Heat Sources on the Dynamics of the Ultra-Long Waves," *Tellus*, Vol. 21, No. 1, Stockholm, Sweden, **1969**, pp. 25–39.

Fujita, Tetsuya, "Advance of Season in View of Upper Planetary Waves," *Papers in Meteorology and Geophysics*, Vol. 7, No. 1, Tokyo Meteorological Research Institute, Japan, Apr. **1956**, pp. 7–28.

Gates, W. Lawrence, "The Stability Properties and Energy Transformations of the Two-Layer Model of Variable Static Stability," *Tellus*, Vol. 13, No. 4, Stockholm, Sweden, Nov. **1961**, pp. 460–471.

Haltiner, G. J., "The Effects of Sensible Heat Exchange on the Dynamics of Baroclinic Waves, " *Tellus*, Vol. 19, No. 2, Stockholm, Sweden, **1967**, pp. 183–198.

Kindle, E. C., Haws, R. C., and Browning, R. H., "Three-Dimensional Analysis of Mid-Latitude Diabatic Heating and Significance to Dynamic Prediction," paper presented at the AMS Conference on Physical Processes of the Lower Atmosphere, Ann Arbor, Mich., Mar. 20–22, **1967**, 38 pp, available from Research Triangle Institute, Research Triangle Park, N.C.

Murakami, Takio, "Vertical Transfer of Energy Due to Stationary Disturbances Induced by Topography and Diabatic Heat Sources and Sinks," *Journal of the Meteorological Society of Japan*, Ser. 2, Vol. 45, No. 3, Tokyo, June **1967**, pp. 205–231.

Ninomiya, K., "Heat Budget Over the Japan Sea and the Japan Islands During the Period of Heavy Snow Storm," *Papers in Meteorology and Geophysics*, Vol. 15, No. 1, Tokyo Meteorological Research Institute, Japan, Apr. **1964**, pp. 52–70.

Ogura, Y., "Wave Solutions of the Vorticity Equation for the 2½-Dimensional Model," *Journal of Meteorology*, Vol. 14, No. 1, Feb. **1957**, pp. 60–64.

Smagorinsky, Joseph, "The Dynamical Influence of Large-Scale Heat Sources and Sinks on the Quasi-Stationary Mean Motions of the Atmosphere," *Quarterly Journal of the Royal Meteorological Society*, Vol. 79, No. 341, London, England, July **1953**, pp. 342–366.

Vukovich, Fred, M., and Chow, Chi F., "A Study of the Influence of Changes of the Heat Function on Climatic Changes," *Proceedings of the First National Conference on Weather Modification, Albany, New York, April 28–May 1, 1968*, American Meteorological Society, Boston, Mass., **1968***a*, pp. 136–148.

Vukovich, Fred M., and Chow, Chi F., "Research in Numerical, Dynamical, and Operational Weather Forecast Procedures," *Final Report*, Contract No. AF19(628)–5834, Air Force Cambridge Research Laboratories, Bedford, Mass., Apr. **1968***b*, 89 pp.

Wiin-Nielsen, A., "A Note on the Behavior of Very Long Waves in Simple Baroclinic Models," *Journal of Meteorology*, Vol. 18, No. 2, Apr. **1961**, pp. 204–207.

*[Received August 6, 1971; revised February 11, 1972]*